

IFUP-TH 25/96
May 1996
gr-qc/9605072

Spectrum of relic gravitational waves in string cosmology

Alessandra Buonanno, Michele Maggiore and Carlo Ungarelli

Dipartimento di Fisica dell'Università and INFN,
piazza Torricelli 2, I-56100 Pisa, Italy.

Abstract. We compute the spectrum of relic gravitons in a model of string cosmology. In the low- and in the high-frequency limits we reproduce known results. The full spectrum, however, also displays a series of oscillations which could give a characteristic signature at the planned LIGO/VIRGO detectors. For special values of the parameters of the model the signal reaches its maximum already at frequencies accessible to LIGO and VIRGO and it is close to the sensitivity of first generation experiments.

arXiv:gr-qc/9605072v1 31 May 1996

1 Introduction

In the next few years a number of detectors for gravitational waves, and in particular the LIGO and VIRGO interferometers, are expected to start operating in a range of frequencies between 10 Hz and 1 kHz. One of the possible signals which could be searched, correlating the output of two detectors, is a stochastic background of gravitational waves. This background is expected to have different components, with different origin: it will get contributions from a large number of unresolved sources at modest red-shifts, as well as from radiation of cosmological origin. The latter is especially interesting, since it would carry informations about the state of the very early universe.

The basic mechanism of generation of relic gravitational waves in cosmology has been discussed in a number of papers, see e.g. refs. [1, 2], the reviews [3, 4] and references therein. The spectrum can be conveniently expressed using

$$\Omega_{\text{gw}}(f) = \frac{1}{\rho_c} \frac{d\rho_{\text{gw}}}{d \log f}$$

where ρ_c is the critical density of the universe, ρ_{gw} is the energy density in gravitational waves and f is the frequency. Particular attention has been paid to the spectrum produced in inflationary cosmology. In this case one finds that Ω_{gw} decreases with frequency as f^{-2} from 10^{-18} Hz to 10^{-16} Hz, and then it is flat up to a maximum cutoff frequency $f \sim 10^{10}$ Hz. While the frequency dependence of $\Omega_{\text{gw}}(f)$ is fixed, its magnitude depends on a parameter of the model, the Hubble constant during inflation. An upper bound on the spectrum can be obtained from the measurement of COBE of the anisotropy of the microwave background radiation. Via the Sachs-Wolfe effect, a large energy density in gravitational waves at wavelengths comparable to the present Hubble radius would produce fluctuations in the temperature of the photon cosmic background. This gives a limit on Ω_{gw} [5] of about $8 \cdot 10^{-14}$ at $f \sim 10^{-16}$ Hz. Since for larger frequencies the spectrum predicted by inflation is flat, this bound also holds at the frequencies of interest for LIGO and VIRGO. The planned sensitivities of these experiments to a stochastic background are of the order of $\Omega_{\text{gw}} \sim 5 \cdot 10^{-6}$, while the advanced LIGO project aims at $5 \cdot 10^{-11}$ [5]. In any case, the spectrum predicted by these inflationary models is too low to be observed.

Clearly, in order to have a stochastic background which satisfies the COBE bound, but still has a chance of being observable at LIGO or VIRGO, the spectrum must grow with frequency. A spectrum of this type has been found in ref. [6] in a cosmological model suggested by string theory [7, 8, 9]. Because of its fast ($\sim f^3$) growth with frequency at low f , the COBE bound is easily evaded, and the most relevant bound for this type of spectrum comes from nucleosynthesis. The result is that, for a certain range of values of the parameters of the model, the spectrum might be accessible at the interferometer experiments, at least at the advanced level, while satisfying the existing experimental bounds.

In ref. [6] this spectrum has been estimated, using approximate methods, in the low- and in the high-frequency limits, and neglecting overall numerical factors. In this paper we present a detailed computation of the spectrum, solving exactly the relevant differential equations. We fix the numerical factors and we present the frequency dependence in the intermediate region. The latter displays an interesting feature: it shows a series of oscillations, which might provide a characteristic experimental signature.

As remarked in [6], one must be aware of the fact that it might not be legitimate to use field-theoretical methods during the 'stringy phase' of the cosmological model, see sect. 2, and large frequencies are indeed sensitive to this phase. However the best one can do, at this stage, is to write down a specific cosmological model and see what are its predictions. Of course, these predictions should only be considered as indicative.

2 The model

The low energy string effective action depends on the metric $g_{\mu\nu}$ and on the dilaton field ϕ (we neglect the antisymmetric tensor field). At lowest order in the derivatives and in e^ϕ it is given by

$$S = -\frac{1}{2\lambda_s^2} \int d^4x \sqrt{-g} \left[e^{-\phi} (R + \partial_\mu \phi \partial^\mu \phi) - V_{\text{dil}}(\phi) \right], \quad (1)$$

where λ_s is the string length and ϕ is the dilaton field. The dilaton potential $V_{\text{dil}}(\phi)$ is due to non-perturbative effects and therefore vanishes as $\exp(-c \exp(-\phi))$ for ϕ large and negative, with c a positive constant. We consider a homogeneous, isotropic and spatially flat background, $\phi = \phi(t)$, $ds^2 = dt^2 - a^2(t) d\mathbf{x}^2$, and we introduce conformal time η , $dt = a(\eta) d\eta$. The pre-big-bang scenario proposed by Gasperini and Veneziano [7, 8, 9] suggests the following choice for the background metric and dilaton field.

For $-\infty < \eta < \eta_s$, with $\eta_s < 0$, we have a dilaton-dominated regime with

$$a(\eta) = -\frac{1}{H_s \eta_s} \left(\frac{\eta - (1 - \alpha)\eta_s}{\alpha \eta_s} \right)^{-\alpha} \quad (2)$$

$$\phi(\eta) = \phi_s - \gamma \log \frac{\eta - (1 - \alpha)\eta_s}{\eta_s}. \quad (3)$$

With the values $\alpha = 1/(1 + \sqrt{3})$, $\gamma = \sqrt{3}$ this is a solution of the equations of motion derived from the effective action (1) in the absence of external matter [7].

At a value $\eta = \eta_s$ the curvature becomes of the order of the string scale, and the lowest order effective action (1) does not give anymore a good description. We are in a full 'stringy' regime. One expects that higher order corrections to the effective action

tame the growth of the curvature, and both $(1/a)da/dt$ and $d\phi/dt$ stay approximately constant. In terms of conformal time, this means

$$a(\eta) = -\frac{1}{H_s \eta}, \quad \phi(\eta) = \phi_s - 2\beta \log \frac{\eta}{\eta_s} \quad (4)$$

The stringy phase lasts for $\eta_s < \eta < \eta_1 < 0$. One then expects that at this stage the dilaton potential becomes operative and, either with a modification of the classical equations of motion due to the dilaton potential [10], or via quantum tunneling [11] the solution joins the standard radiation dominated solution with constant dilaton, which is also a solution of the string equations of motion derived from the action (1), with external bulk stringy matter [7]. This gives, for $\eta_1 < \eta < \eta_r$, (with $\eta_r > 0$)

$$a(\eta) = \frac{1}{H_s \eta_1^2} (\eta - 2\eta_1), \quad \phi = \phi_0. \quad (5)$$

After that, the standard matter dominated era takes place. We have chosen the additive and multiplicative constants in $a(\eta)$ in such a way that $a(\eta)$ and $da/d\eta$ (and therefore also da/dt) are continuous across the transitions.

The equation for the Fourier modes of metric tensor perturbations for the two physical polarizations in the transverse traceless gauge is [12]

$$\frac{d^2 \psi_k}{d\eta^2} + [k^2 - V(\eta)] \psi_k = 0, \quad (6)$$

$$V(\eta) = \frac{1}{a} e^{\phi/2} \frac{d^2}{d\eta^2} (a e^{-\phi/2}). \quad (7)$$

Inserting the expressions (2-5) the potential is

$$\begin{aligned} V(\eta) &= \frac{1}{4} (4\nu^2 - 1) (\eta - (1 - \alpha)\eta_s)^{-2}, & -\infty < \eta < \eta_s \\ V(\eta) &= \frac{1}{4} (4\mu^2 - 1) \eta^{-2}, & \eta_s < \eta < \eta_1 \\ V(\eta) &= 0, & \eta_1 < \eta < \eta_r \end{aligned} \quad (8)$$

where $2\mu = |2\beta - 3|$, $2\nu = |2\alpha - \gamma + 1|$. The exact solutions of eq. (6) in the three regions are

$$\begin{aligned} \psi_k(\eta) &= \sqrt{|\eta - (1 - \alpha)\eta_s|} C H_\nu^{(2)}(k|\eta - (1 - \alpha)\eta_s|), & -\infty < \eta < \eta_s \\ \psi_k(\eta) &= \sqrt{|\eta|} [A_+ H_\mu^{(2)}(k|\eta|) + A_- H_\mu^{(1)}(k|\eta|)], & \eta_s < \eta < \eta_1 \\ \psi_k(\eta) &= i \sqrt{\frac{2}{\pi k}} [B_+ e^{ik\eta} - B_- e^{-ik\eta}], & \eta_1 < \eta < \eta_r \end{aligned} \quad (9)$$

where $H_\nu^{(1,2)}$ are Hankel's functions. The constants A_\pm, B_\pm can be obtained requiring the continuity of the solution and of its derivative. We have chosen the boundary conditions so that, at $\eta \rightarrow -\infty$, $\psi_k \sim \exp(ik\eta)$. In this case the number of particles created per unit cell of the phase space is given by $|B_-|^2$.

Before performing the matching, let us discuss the parameters of the model. The two constants α, γ parametrize the solution in the dilaton dominated phase and therefore they are fixed by the effective action (1): $\alpha = 1/(1 + \sqrt{3}), \gamma = \sqrt{3}$ and then $\nu = 0$ (anyway, we will write many of our results for generic ν). Instead μ (or β) is a free parameter which measures the growth of the dilaton during the stringy phase; by definition $\mu \geq 0$. The parameter H_s is the Hubble constant during the stringy phase. Since in this model the growth of the curvature can only be stopped by the inclusion of higher order terms in the string effective action, it is clear that the natural value for H_s is of the order of the inverse of the string length λ_s . If one uses the value $\lambda_s^2 \simeq (2/\alpha_{GUT}) L_{\text{Pl}}^2 \simeq 40 L_{\text{Pl}}^2$ then the typical value of H_s is $H_s \simeq 1/\lambda_s \simeq 0.15 M_{\text{Pl}}$ where M_{Pl} is the Planck mass. Finally, there are the two parameters η_s, η_1 . In the solution for ψ_k , and therefore in the spectrum, they appear in the combinations $k|\eta_s|, k|\eta_1|$, where k is the comoving wave number. If we denote by $2\pi f$ the physical frequency observed at a detector, we have $2\pi f = k/a(t_{\text{pres}})$, where t_{pres} is the present value of cosmic time. Therefore, using eq. (4),

$$k|\eta_1| = 2\pi f a(t_{\text{pres}})|\eta_1| = \frac{2\pi f}{H_s} \frac{a(t_{\text{pres}})}{a(t_1)} = \frac{2\pi f}{H_s} \left(\frac{t_{\text{pres}}}{t_{\text{eq}}}\right)^{2/3} \left(\frac{t_{\text{eq}}}{t_1}\right)^{1/2}, \quad (10)$$

where $t_{\text{eq}} \simeq 3.4 \cdot 10^{10} h_0^{-4} s$ is the time of matter-radiation equilibrium, and $t_{\text{pres}} = 2/(3H_0) \simeq 2.1 \cdot 10^{17} h_0^{-1} s$. The constant h_0 parametrizes the uncertainty in the present value of the Hubble constant $H_0 = 3.2 \cdot 10^{-18} h_0 \text{ Hz}$, and it cancels in eq. (10); t_1 is the value of cosmic time when the string phase ends. In this context, the natural choice is $t_1 \simeq \lambda_s$. Therefore the parameter η_1 can be traded for a parameter f_1 defined by

$$k|\eta_1| = \frac{f}{f_1}, \quad f_1 \simeq 4.3 \cdot 10^{10} \text{ Hz} \left(\frac{H_s}{0.15 M_{\text{Pl}}}\right) \left(\frac{t_1}{\lambda_s}\right)^{1/2}. \quad (11)$$

The order of magnitude of f_1 is therefore fixed. Note that at the frequencies of interest for LIGO and VIRGO f ranges between 10 Hz and 1 kHz, and f/f_1 is a very small quantity. Similarly we can introduce a parameter f_s instead of η_s , from $k|\eta_s| = f/f_s$. This parameter depends on the duration of the string phase, and it is therefore totally unknown, even as an order of magnitude. However, since $|\eta_1| < |\eta_s|$, we have $f_s < f_1$.

To summarize, the model has a dimensionful parameter f_s , which can have any value in the range $0 < f_s < f_1$ and a dimensionless parameter $\mu \geq 0$ (or equivalently β with $2\mu = |2\beta - 3|$). The dimensionless constants α, ν are fixed, $\alpha = 1/(1 + \sqrt{3}), \nu = 0$ and the dimensionful constants H_s, f_1 are fixed within an uncertainty of about one or two orders of magnitude. The constant ϕ_s appearing in eq. (2) drops out from the potential, eq. (7), and it is therefore irrelevant for our purposes.¹

¹For comparison, in ref. [6] the two parameters which are not fixed are chosen as g_s/g_1 , which in

3 The spectrum

Performing the matching at $\eta = \eta_s$ we get

$$A_{\pm} = \pm i \frac{\pi x_s \sqrt{\alpha}}{4} \left[H_{\nu}^{(2)'}(\alpha x_s) H_{\mu}^{(1,2)}(x_s) - H_{\nu}^{(2)}(\alpha x_s) H_{\mu}^{(1,2)'}(x_s) \right. \\ \left. + \frac{1}{2x_s} \frac{1-\alpha}{\alpha} H_{\nu}^{(2)}(\alpha x_s) H_{\mu}^{(1,2)}(x_s) \right], \quad (12)$$

where $x_s = f/f_s$; in $H_{\mu}^{(1,2)}(x_s)$, $H_{\mu}^{(1)}(x_s)$ refers to A_+ and $H_{\mu}^{(2)}(x_s)$ refers to A_- . In deriving these expressions we have used the identity between Hankel functions $H_{\nu}^{(2)'}(x) H_{\nu}^{(1)}(x) - H_{\nu}^{(1)'}(x) H_{\nu}^{(2)}(x) = -4i/(\pi x)$. The constant C appearing in eq. (9) has been fixed requiring $|A_+|^2 - |A_-|^2 = 1$, which gives $|C| = 1$. Next we perform the matching at $\eta = \eta_1$. However, at the frequencies of interest for LIGO and VIRGO, $k|\eta_1| = f/f_1 = O(10^{-8})$, and therefore in this second matching we can use the small argument limit of the Hankel functions, with a totally negligible error. This gives a relatively simple analytical expression for the coefficient B_- which, apart from an irrelevant overall phase, is, for $\mu \neq 0$,²

$$B_- = \sqrt{\pi\alpha} \frac{2\mu-1}{8} \Gamma(\mu) \left(\frac{f}{2f_s} \right) \left(\frac{f}{2f_1} \right)^{-\mu-1/2} \left[H_{\nu}^{(2)'} \left(\frac{\alpha f}{f_s} \right) J_{\mu} \left(\frac{f}{f_s} \right) \right. \\ \left. - H_{\nu}^{(2)} \left(\frac{\alpha f}{f_s} \right) J'_{\mu} \left(\frac{f}{f_s} \right) + \frac{(1-\alpha)}{2\alpha} \frac{f_s}{f} H_{\nu}^{(2)} \left(\frac{\alpha f}{f_s} \right) J_{\mu} \left(\frac{f}{f_s} \right) \right], \quad (13)$$

where $J_{\mu}(z)$ is the Bessel function. The spectrum of gravitational waves is expressed with the quantity

$$\Omega_{\text{gw}}(f) = \frac{1}{\rho_c} \frac{d\rho_{\text{gw}}}{d \log f} = \frac{1}{\rho_c} 16\pi^2 f^4 |B_-|^2 \quad (14)$$

where $\rho_c = 3H_0^2 M_{\text{pl}}^2 / (8\pi)$. Then our result for the spectrum is

$$\Omega_{\text{gw}}(f) = a(\mu) \frac{(2\pi f_s)^4}{H_0^2 M_{\text{pl}}^2} \left(\frac{f_1}{f_s} \right)^{2\mu+1} \left(\frac{f}{f_s} \right)^{5-2\mu} \left| H_{\nu}^{(2)'} \left(\frac{\alpha f}{f_s} \right) J_{\mu} \left(\frac{f}{f_s} \right) \right. \\ \left. - H_{\nu}^{(2)} \left(\frac{\alpha f}{f_s} \right) J'_{\mu} \left(\frac{f}{f_s} \right) + \frac{(1-\alpha)}{2\alpha} \frac{f_s}{f} H_{\nu}^{(2)} \left(\frac{\alpha f}{f_s} \right) J_{\mu} \left(\frac{f}{f_s} \right) \right|^2 \quad (15)$$

where

$$a(\mu) = \frac{\alpha}{48} 2^{2\mu} (2\mu-1)^2 \Gamma^2(\mu). \quad (16)$$

our notations is $(f_s/f_1)^{\beta}$, and $z_s = f_1/f_s$.

²For $\mu = 0$ the small argument limit of the Hankel function is different. The result for $\mu = 0$ is the same as eq. (13) if one writes $2 \log f/f_1$ instead of $\Gamma(\mu)$ and sets $\mu = 0$ in the remaining expression. In the following we write our formulae for $\mu \neq 0$.

In the most interesting case $\nu = 0$, using the identity $H_0^{(2)'}(z) = -H_1^{(2)}(z)$, we can rewrite the spectrum as

$$\begin{aligned} \Omega_{\text{gw}}(f) = & a(\mu) \frac{(2\pi f_s)^4}{H_0^2 M_{\text{pl}}^2} \left(\frac{f_1}{f_s}\right)^{2\mu+1} \left(\frac{f}{f_s}\right)^{5-2\mu} \left| H_0^{(2)}\left(\frac{\alpha f}{f_s}\right) J'_\mu\left(\frac{f}{f_s}\right) + \right. \\ & \left. + H_1^{(2)}\left(\frac{\alpha f}{f_s}\right) J_\mu\left(\frac{f}{f_s}\right) - \frac{(1-\alpha)}{2\alpha} \frac{f_s}{f} H_0^{(2)}\left(\frac{\alpha f}{f_s}\right) J_\mu\left(\frac{f}{f_s}\right) \right|^2. \end{aligned} \quad (17)$$

Expanding our exact expression for small values of f/f_s we get, for $\nu = 0$,

$$\begin{aligned} \Omega_{\text{gw}}(f) \simeq & \frac{(2\mu-1)^2}{192\mu^2\alpha} \frac{(2\pi f_s)^4}{H_0^2 M_{\text{pl}}^2} \left(\frac{f_1}{f_s}\right)^{2\mu+1} \left(\frac{f}{f_s}\right)^3 \times \\ & \left\{ (2\mu\alpha - 1 + \alpha)^2 + \frac{4}{\pi^2} \left[(2\mu\alpha - 1 + \alpha) \left(\log \frac{\alpha f}{2f_s} + \gamma_E \right) - 2 \right]^2 \right\}, \end{aligned} \quad (18)$$

where $\gamma_E \simeq 0.5772\dots$ is Euler constant. This expression agrees with the result obtained in the literature, see eq. (5.7) of ref. [9], apart for the numerical constants which cannot be computed using only the approximate solution discussed in refs. [9, 6].

Let us observe that the low frequency limit in which eq. (18) holds is actually $f \ll f_s \ll f_1$. If we are interested in the limit $f \ll f_s \sim f_1$ we should not take the small argument limit of the Hankel function when performing the matching at η_1 . Rather, we must keep the exact expression and perform the expansion in the final result. If we do not make any assumption on the value of f_1/f_s a straightforward computation shows that in the limit $f/f_s \ll 1, f/f_1 \ll 1$

$$\begin{aligned} B_- \simeq & \frac{1}{4\mu\sqrt{\pi\alpha}} \times \\ & \left\{ \left(\mu - \frac{1}{2} \right) \left[1 + \frac{i\pi}{4} (1 - \alpha - 2\mu\alpha) \left(1 - \frac{2i}{\pi} \left(\log \frac{\alpha f}{2f_s} + \gamma_E \right) \right) \right] \left(\frac{f}{2f_s} \right)^\mu \left(\frac{f}{2f_1} \right)^{-\mu-1/2} \right. \\ & \left. + \left(\mu + \frac{1}{2} \right) \left[1 + \frac{i\pi}{4} (1 - \alpha + 2\mu\alpha) \left(1 - \frac{2i}{\pi} \left(\log \frac{\alpha f}{2f_s} + \gamma_E \right) \right) \right] \left(\frac{f}{2f_s} \right)^{-\mu} \left(\frac{f}{2f_1} \right)^{\mu-1/2} \right\} \end{aligned}$$

from which we derive again eq. (18) if we now take $f_s \ll f_1$. As we will see below, the graviton spectrum is negligibly small unless $f_s \ll f_1$, so the physically relevant limit is the one which leads to eq. (18). If we instead consider the spectrum with $\nu > 0$ a simple calculation gives a low frequency behavior $\sim f^{3-2\nu}$, without logarithmic corrections (the absence of the $\log f$ term is due to the different small argument limit of $H_\nu^{(1,2)}$ for $\nu = 0$ and for $\nu > 0$.)

Expanding eq. (17) in the limit $f \gg f_s$ (but still $f \ll f_1$ since eq. (17) holds only in this limit) we find instead

$$\Omega_{\text{gw}}(f) \simeq \frac{4a(\mu)}{\pi^2\alpha} \frac{(2\pi f_s)^4}{H_0^2 M_{\text{pl}}^2} \left(\frac{f_1}{f_s}\right)^{2\mu+1} \left(\frac{f}{f_s}\right)^{3-2\mu}$$

$$= \frac{4a(\mu)}{\pi^2\alpha} \frac{(2\pi f_1)^4}{H_0^2 M_{\text{pl}}^2} \left(\frac{f}{f_1}\right)^{3-2\mu} \quad (19)$$

which agrees, in the frequency dependence, with the result of ref. [6].³ It is important to stress that in the high frequency limit the unknown parameter f_s cancels.

Finally, at sufficiently large f , there is a rather sharp cutoff and the spectrum goes to zero exponentially. The cutoff can be obtained computing the spectrum without performing the limit $f \ll f_1$ in the second matching. More simply, the cutoff frequency f_{max} can be estimated from $k_{\text{max}}^2 \simeq |V(\eta_1)|$, which gives

$$f_{\text{max}} \simeq \frac{1}{2} \sqrt{|4\mu^2 - 1|} f_1. \quad (20)$$

4 Discussion

From eq. (19) we see that the form of the spectrum depends crucially on whether $\mu < 3/2$, $\mu = 3/2$ or $\mu > 3/2$. Let us consider first the case $\mu > 3/2$. In this case the spectrum is a decreasing function of f if $f \gg f_s$. Numerically,

$$\frac{(2\pi f_1)^4}{H_0^2 M_{\text{pl}}^2} \simeq 1.4 \cdot 10^{-6} \frac{1}{h_0^2} \left(\frac{H_s}{0.15 M_{\text{pl}}}\right)^4 \left(\frac{t_1}{\lambda_s}\right)^2, \quad (21)$$

and in eq. (19) this number is multiplied by $(f_1/f)^{2\mu-3}$; f_1/f is $O(10^8)$ at $f = 100$ Hz and even larger for smaller frequencies, while $2\mu - 3$ is positive in this case. Therefore, for $\mu > 3/2$, Ω_{gw} would violate any experimental bound. More precisely, the computation becomes invalid because we should include the back-reaction of the produced gravitons on the metric [6]. We will therefore consider only $0 < \mu \leq 3/2$. In this case, the spectrum at low frequencies increases as $\sim f^3 \log^2 f$, and at high frequencies is increasing as $f^{3-2\mu}$ (or going to a constant if $\mu = 3/2$.)

Fig. 1 shows the form of the spectrum for $\mu = 1.4$ and for $\mu = 3/2$. In this figure we plot $\Omega_{\text{gw}}(f)$, measured in units of $a(\mu) \left[(2\pi f_s)^4 / (H_0^2 M_{\text{pl}}^2) \right] (f_1/f_s)^{2\mu+1}$, which is the overall constant appearing in eq. (17), versus f/f_s . We see that, compared to the low- and high-frequency expansions discussed in [6], the spectrum also displays a series of oscillations. Depending on the value of f_s , the window available to the LIGO and VIRGO interferometers, f between 10 Hz and 1 kHz, may contain many oscillations, and this would provide a rather characteristic signature.

To give an idea of the magnitude of the spectrum, in figs. 2 and 3 we plot $h_0^2 \Omega(f)$ for $\mu = 1.4$ and for $\mu = 3/2$, for a specific value of f_s , $f_s = 100$ Hz (this choice of parameters is motivated below), and for $H_s = 0.15 M_{\text{pl}}$ and $t_1 = \lambda_s$, in the frequency range relevant for LIGO and VIRGO. (Note that the quantity of interest for the

³For the comparison with ref. [6], note that, since $2\mu = |2\beta - 3|$, if $2\beta > 3$ the dependence on f is $\sim f^{3-2\mu} = f^{6-2\beta}$ while, if $2\beta < 3$, $f^{3-2\mu} = f^{2\beta}$, which therefore reproduces eq. (3.5) of ref. [6].

experimentalist is not Ω_{gw} but $h_0^2 \Omega_{\text{gw}}$, since h_0 only reflects our uncertainty in the quantity which we use to normalize the result.)

It is also useful to give the result in terms of the quantity $h_c(f)$, which is the dimensionless strain $\Delta L/L$ produced in the arms of the detector, and is related to $\Omega_{\text{gw}}(f)$ by [13]

$$h_c(f) \simeq 1.3 \cdot 10^{-20} \sqrt{h_0^2 \Omega_{\text{gw}}(f)} \left(\frac{100 \text{ Hz}}{f} \right). \quad (22)$$

Fig. 4 shows a plot of $h_c(f)$ versus f for $f_s = 10$ Hz and for $\mu = 3/2$ and $\mu = 1.4$.

Let us then discuss what is the best possible result that we can obtain from this model, varying the two parameters f_s and μ , with $0 < f_s < f_1$ and $0 < \mu \leq 3/2$. Suppose that we want to detect a signal at a given frequency, say $f = 100$ Hz. In fig. 5 we plot Ω_{gw} , from eq. (17), as a function of f_s at fixed f . We see that, independently of μ , it increases for decreasing f_s , and when $f_s \ll f$ it reaches asymptotically the constant value given by eq. (19). So, if we want to detect a signal at a given frequency f , the optimal situation is obtained if the value of f_s is smaller than f . How much smaller is not very important, since as a function of f_s , Ω_{gw} saturates and practically reaches its maximum value as soon as, say, $f_s < 0.5f$. The maximum Ω_{gw} is therefore given by eq. (19), which still depends on the other parameter μ . Since f/f_1 is a very small parameter, we see immediately that the best possible situation is realized when $\mu = 3/2$. Note that this means $\beta = 0$ or $\beta = 3$, and in the first case not only the derivative of the dilaton with respect to cosmic time, but even the dilaton itself stays constant during the stringy phase.

In this case, Ω_{gw} reaches a maximum value

$$h_0^2 \Omega_{\text{gw}}^{\text{max}} = \frac{2h_0^2}{3\pi} \frac{(2\pi f_1)^4}{H_0^2 M_{\text{pl}}^2} \simeq 3.0 \cdot 10^{-7} \left(\frac{H_s}{0.15 M_{\text{pl}}} \right)^4 \left(\frac{t_1}{\lambda_s} \right)^2. \quad (23)$$

If $\mu = 3/2$, this maximum value is reached as long as $f > f_s$ and therefore, if f_s is smaller than, say, 10 Hz, it is already reached in the VIRGO/LIGO frequency range; after that, the signal oscillates around a constant value (fig. 3). If instead $\mu < 3/2$, eq. (19) shows that there is a further suppression factor $(f/f_1)^{3-2\mu}$, and therefore the maximum value is reached only at the cutoff frequency $f_{\text{max}} \sim f_1$, that is for frequencies around 10 or 100 GHz. However, if μ is not close enough to $3/2$, the suppression factor $(f/f_1)^{3-2\mu}$ makes the signal very small at LIGO/VIRGO frequencies, unless one uses unnaturally large values of H_s, t_1 (fig. 2).

Let us then discuss whether this maximum value is compatible with the experimental constraints mentioned in the Introduction.

We consider first the nucleosynthesis bound [5, 14]

$$\int \Omega_{\text{gw}}(f) d(\log f) \leq \frac{7}{43} (N_\nu - 3) (1 + z_{\text{eq}})^{-1}, \quad (24)$$

where $1 + z_{\text{eq}} \simeq 2.32 \times 10^4 h_0^2$ is the redshift at the time of radiation-matter equilibrium and N_ν is the equivalent number of neutrino species [15]. Using the recent analysis

of ref. [16], $N_\nu < 3.9$, we get

$$\int h_0^2 \Omega_{\text{gw}}(f) d(\log f) < 6.3 \cdot 10^{-6}. \quad (25)$$

For $\mu = 3/2$, Ω_{gw} reaches its maximum value at $f \sim f_s$ and stays approximately constant until the cutoff at $f \sim f_1$ is reached, and therefore the bound gives

$$h_0^2 \Omega_{\text{gw}}^{\text{max}} \log \frac{f_1}{f_s} \lesssim 6.3 \cdot 10^{-6}, \quad (26)$$

If we take $f_s \sim 100$ Hz (which still satisfies $f_s < f$ at the frequency $f = 1$ kHz accessible to LIGO and VIRGO, so that eq. (23) applies), eq. (26) gives an upper bound on the spectrum predicted by string cosmology

$$h_0^2 \Omega_{\text{gw}}^{\text{max}} < 3.2 \cdot 10^{-7}, \quad (27)$$

which can be obtained from eq. (23) with very natural values of H_s, t_1 . This number is smaller than the planned sensitivity of the LIGO and VIRGO detectors in a first phase but well within the planned sensitivity of the advanced project. Smaller values of f_s give a more stringent bound, but the dependence is only logarithmic: if $f_s \sim 10^{-7}$ Hz, the maximum value of $h_0^2 \Omega_{\text{gw}}$ is $1.5 \cdot 10^{-7}$.

The bound from μ sec pulsars is [5]

$$h_0^2 \Omega_{\text{gw}}(f = 10^{-8}\text{Hz}) < 10^{-8}. \quad (28)$$

From fig. 2 we see that, in order to suppress the result at $f = 10^{-8}\text{Hz}$, we must have $f_s \gg 10^{-8}\text{Hz}$, which is well compatible with the condition $f_s \lesssim 10^2$ Hz required before. Even if at $f \sim 1$ kHz we have $h_0^2 \Omega_{\text{gw}}^{\text{max}} = 3.2 \cdot 10^{-7}$, at $f \ll f_s$ we get

$$h_0^2 \Omega_{\text{gw}} \simeq 3.3 \cdot 10^{-9} \left(\frac{f}{f_s} \right)^3 \log^2 \frac{f}{f_s}. \quad (29)$$

We see that a value of, say, $f_s > 10^{-7}$ Hz is sufficient to bring $\Omega_{\text{gw}}(f = 10^{-8}\text{Hz})$ well below the experimental bound. The COBE bound is even more easily satisfied since if $f_s > 10^{-7}$ Hz the value of Ω_{gw} at $f = 10^{-16}$ Hz is totally negligible. Fig. 6 shows the spectrum for $f_s = 100$ Hz and $\mu = 3/2$ in a large range of frequencies, and compares it to the experimental bounds.

In conclusion, in the most favourable case $\mu = 3/2$ and $10^{-7}\text{Hz} < f_s \lesssim 100$ Hz, the relic gravitational waves background predicted by string cosmology at the frequencies of LIGO and VIRGO is about $h_0^2 \Omega_{\text{gw}}^{\text{max}} = 3.2 \cdot 10^{-7}$, which is smaller than the planned sensitivity for coincidence experiments with interferometers in the first phase, but well within the sensitivity at which the advanced LIGO project aims. This maximum value of Ω_{gw} might also be comparable to the sensitivities which could be reached correlating resonant bar detectors such as EXPLORER, NAUTILUS and AURIGA [17]. At the same time, the spectrum satisfies the existing experimental bounds.

Acknowledgements

We are grateful to Maurizio Gasperini and Gabriele Veneziano for very useful comments.

References

- [1] L.P. Grishchuk, Sov. Phys. JETP, 40 (1975) 409.
- [2] A. Starobinski, JETP Lett. 30 (1979) 682;
V. Rubakov, M. Sazhin and A. Veryaskin, Phys. Lett. 115B (1982) 189;
R. Fabbri and M.D. Pollock, Phys. Lett. 125B (1983) 445;
L. Abbott and M. Wise, Nucl. Phys. B244 (1984) 541.
L. Abbott and D. Harari, Nucl. Phys. B264 (1986) 487.
B. Allen, Phys. Rev. D37 (1988) 2078.
- [3] L.P. Grishchuk, Class. Quantum Grav. 10 (1993) 2449.
- [4] V.F. Mukhanov, H.A. Feldman and R.H. Brandenberger, Phys. Rep. 215 (1992) 203.
- [5] B. Allen, “*The Stochastic Gravity-Wave Background: Sources and Detection*”, gr-qc 9604033.
- [6] R. Brustein, M. Gasperini, M. Giovannini and G. Veneziano, Phys. Lett. B361 (1995) 45.
- [7] M. Gasperini and G. Veneziano, Astropart. Phys. 1 (1993) 317; Mod. Phys. Lett. A8 (1993) 3701; Phys. Rev. D50 (1994) 2519.
- [8] G. Veneziano, “*String Cosmology: Basic Ideas and General Results*”, in “*String Gravity and Physics at the Planck Energy Scale*”, N. Sanchez and A. Zichichi eds., Kluwer Publ., pag 285.
- [9] M. Gasperini, “*Status of String Cosmology: Phenomenological Aspects*”, in “*String Gravity and Physics at the Planck Energy Scale*”, N. Sanchez and A. Zichichi eds., Kluwer Publ., pag 305.
- [10] R. Brustein and G. Veneziano, Phys. Lett. B329 (1994) 429.
- [11] M. Gasperini, J. Maharana and G. Veneziano, “*Graceful exit in quantum string cosmology*”, Cern-Th/96-32; hep-th/9602087, Nucl. Phys. B, in press.
M. Gasperini and G. Veneziano, “*Birth of the Universe as quantum scattering in string cosmology*”, Cern-Th/96-49, hep-th/9602096, Gen. Rel. Grav., in press.
- [12] M. Gasperini and M. Giovannini, Phys. Rev. D47 (1993) 1519.
- [13] K. S. Thorne, in “*300 Years of Gravitation*”, S. Hawking and W. Israel eds., Cambridge Univ. Press, 1987.

- [14] R. Brustein, M. Gasperini and G. Veneziano, “*Peak and End Point of the Relic Graviton Background in String Cosmology*”, preprint CERN-TH/96-37, hep-th/9604084.
- [15] E. Kolb and R. Turner, “*The Early Universe*”, Addison-Wesley Publ., 1990
- [16] C. Copi et al., Phys. Rev. Lett. 75 (1995) 3981.
- [17] M. Cerdonio et al., “*Status of the Auriga Gravitational Wave Antenna and Perspectives for the Gravitational Waves Search with Ultracryogenic Resonant Mass Detectors*”, in “Proc. of the First Edoardo Amaldi Conference”, ed. by E. Coccia, G. Pizzella and F. Ronga (World Scientific, Singapore, 1995).
P. Astone et al., “*Upper limit for a gravitational wave stochastic background measured with the EXPLORER and NAUTILUS gravitational wave resonant detectors*”, (Rome, February 1996), to appear.

Figure captions

Fig. 1 Ω_{gw} , measured in units of $a(\mu)((2\pi f_s)^4/(H_0^2 M_{\text{pl}}^2))(f_1/f_s)^{2\mu+1}$ vs. f/f_s for $\mu = 1.4$ and $\mu = 1.5$.

Fig. 2 $\Omega_{\text{gw}}(f)$ vs. f for $\mu = 1.4$, $f_s = 100$ Hz and $f_1 = 4.3 \cdot 10^{10}$ Hz; for comparison we also show the low- and high-frequencies limits.

Fig. 3 $\Omega_{\text{gw}}(f)$ vs. f for $\mu = 1.5$, $f_s = 100$ Hz and $f_1 = 4.3 \cdot 10^{10}$ Hz; for comparison we also show the low- and high-frequencies limits.

Fig. 4 $h_c(f)$ vs. f for $\mu = 1.5$ and $\mu = 1.4$, $f_s = 10$ Hz and $f_1 = 4.3 \cdot 10^{10}$ Hz.

Fig. 5 Ω_{gw} vs. f_s for $\mu = 1.4$, at fixed $f = 100$ Hz and $f_1 = 4.3 \cdot 10^{10}$ Hz.

Fig. 6 $\Omega_{\text{gw}}(f)$ vs. f for $\mu = 1.5$, $f_s = 10$ Hz and $f_1 = 4.3 \cdot 10^{10}$ Hz compared to the experimental bounds.

Fig. 1

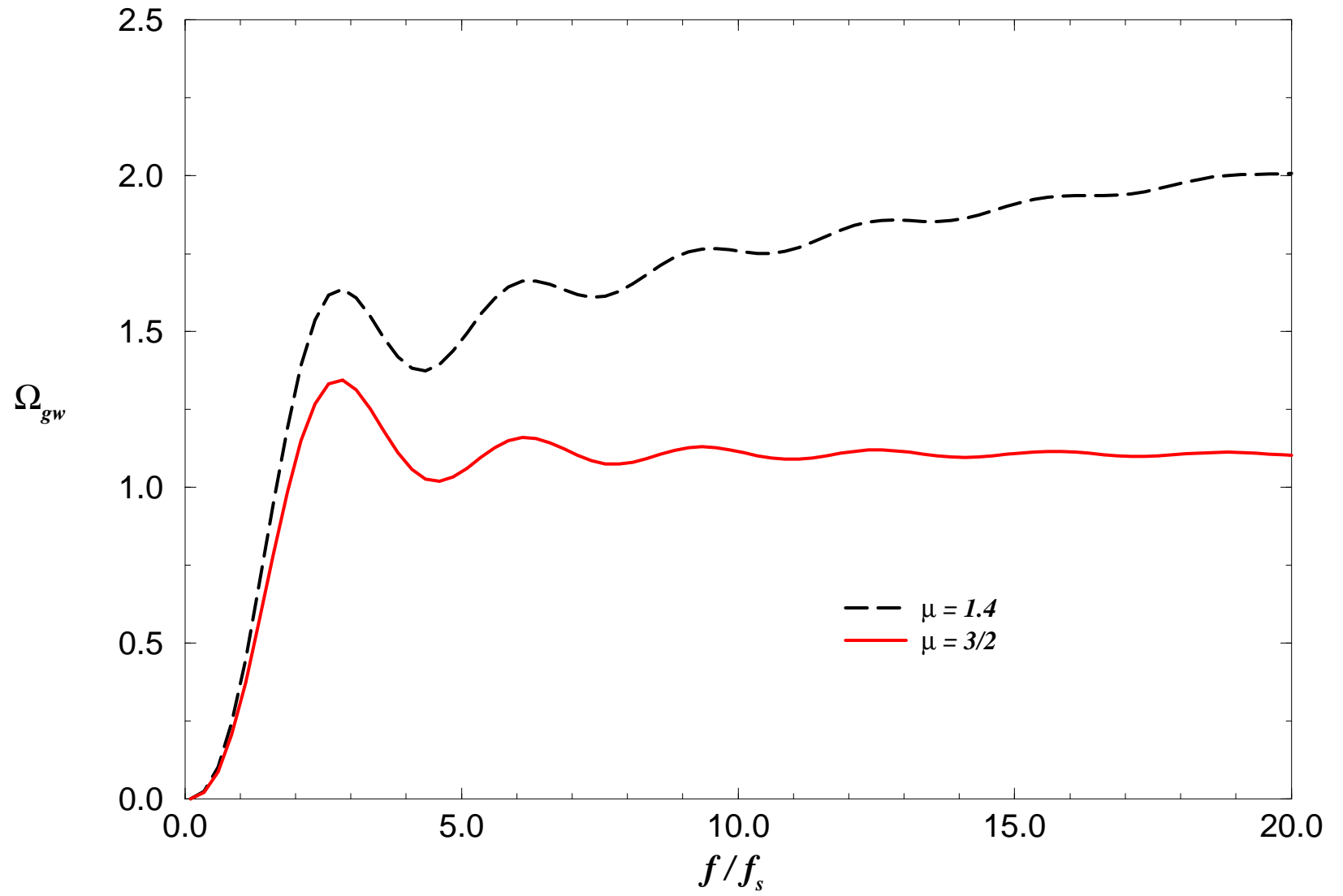


Fig. 2

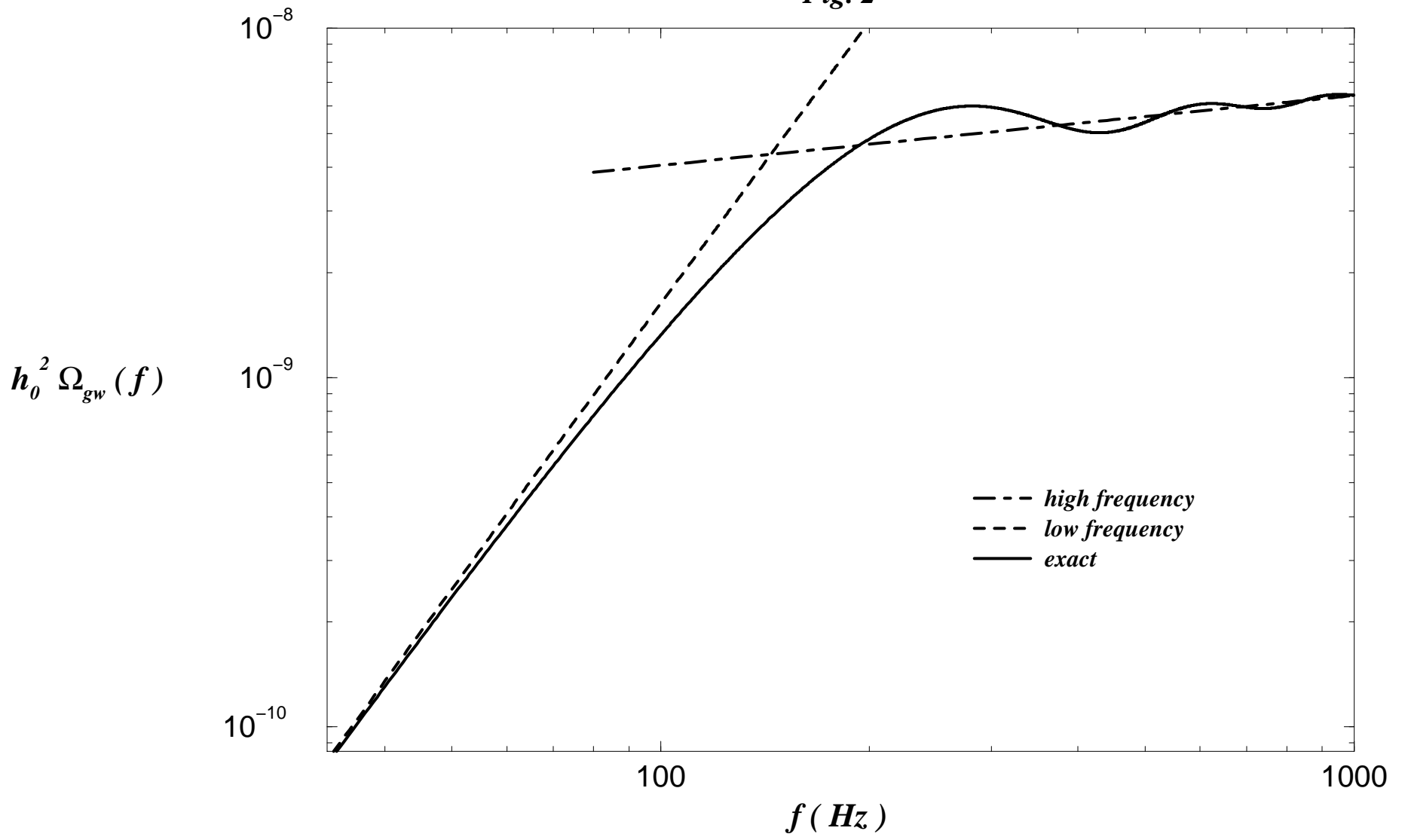


Fig. 3

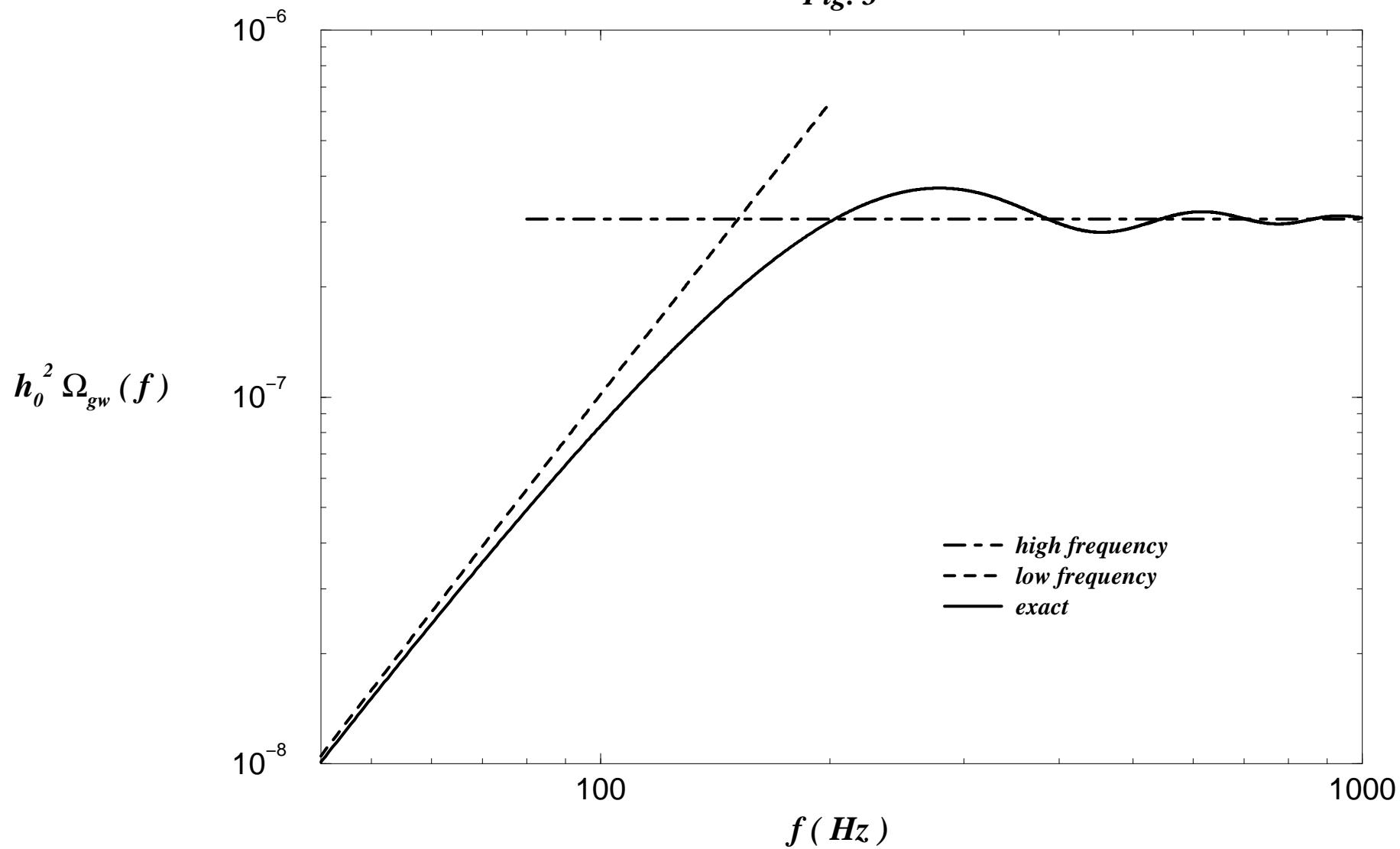


Fig. 4

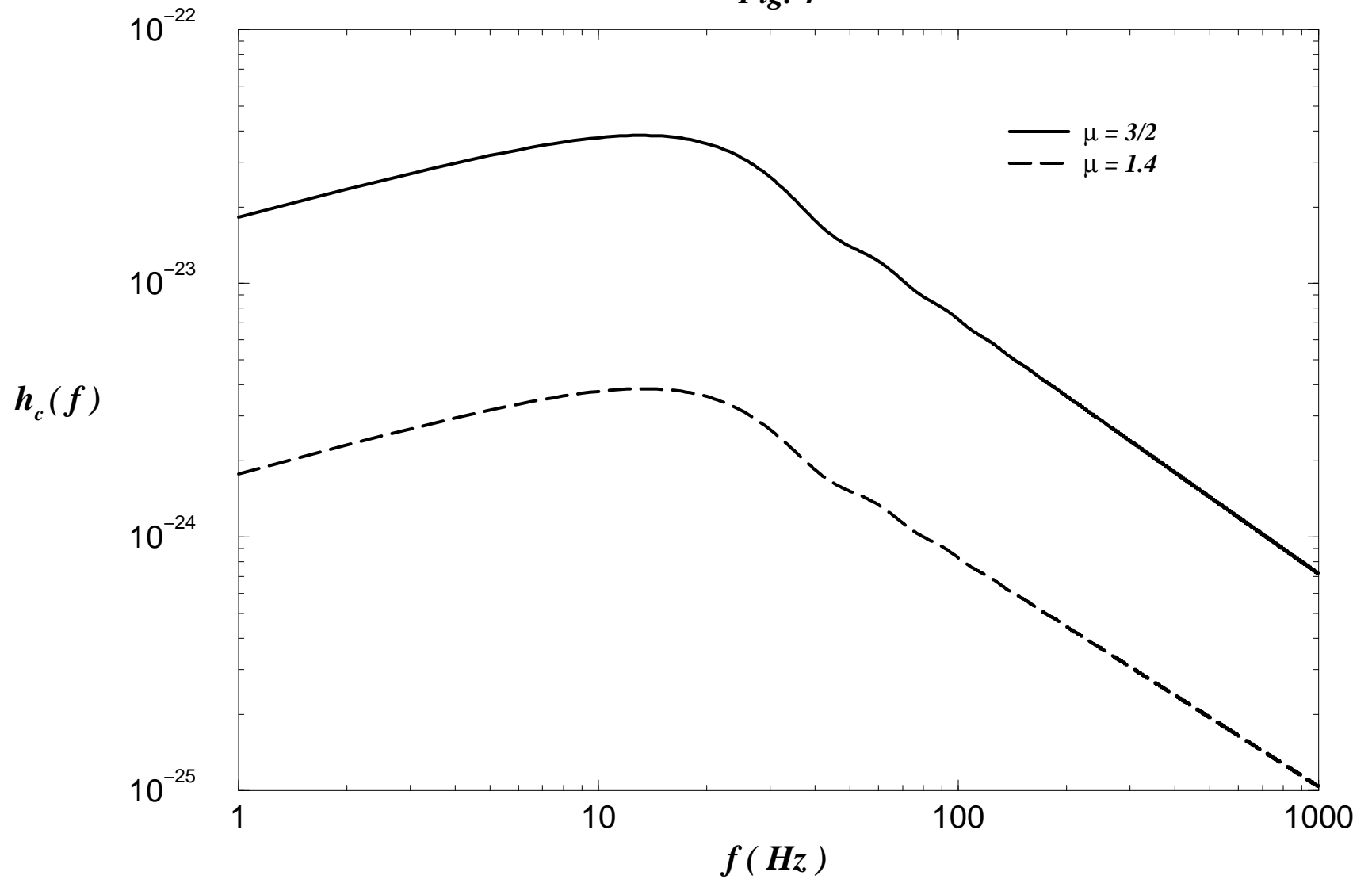


Fig. 5

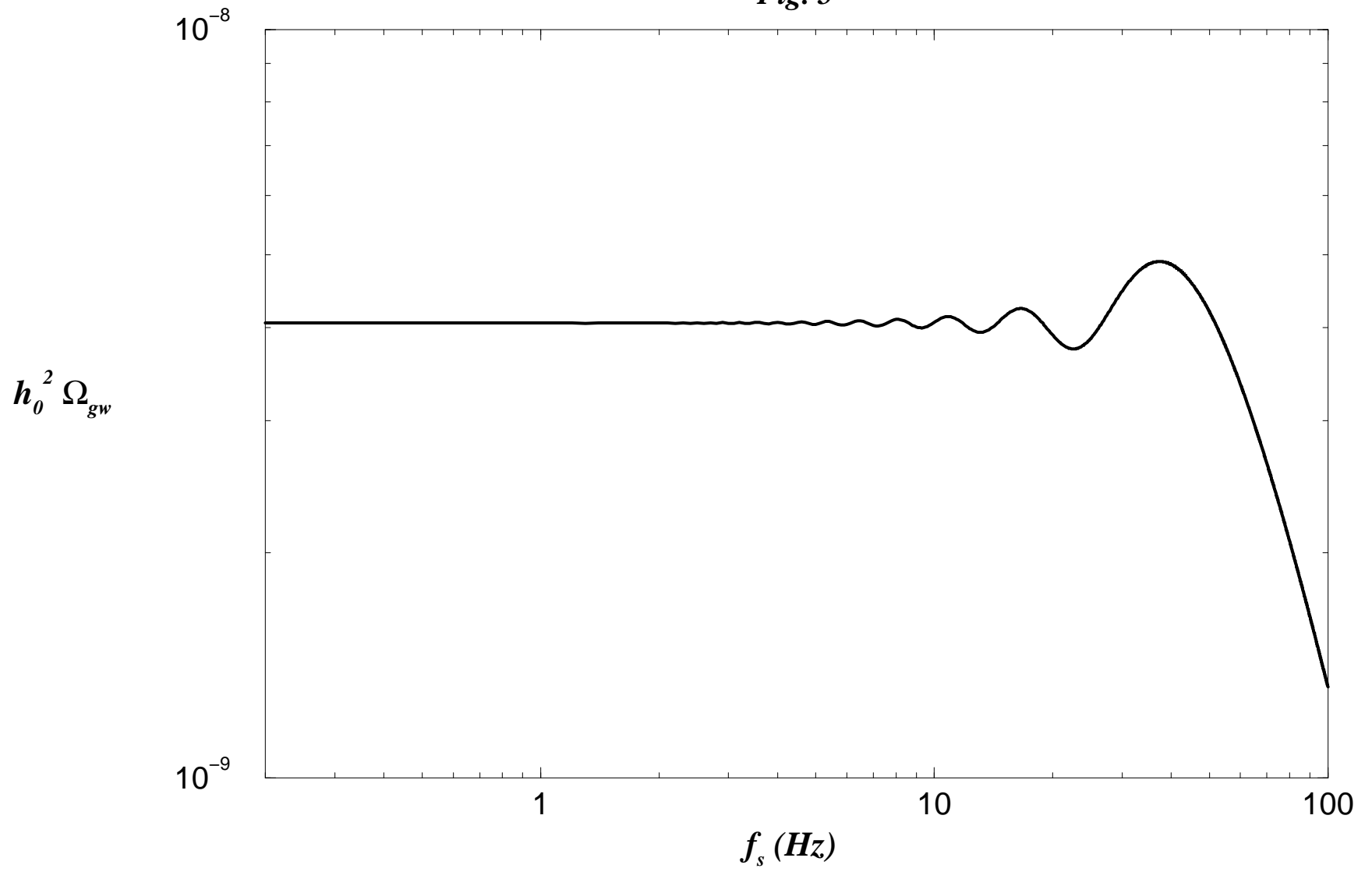


Fig. 6

